

FLUID DYNAMICS AND THERMODYNAMICS NUMERICAL MODELLING  
OF SELF-HEALING FIBRE REINFORCED LAMINATED COMPOSITES

KAM CHEE ZHOU

UNIVERSITI TEKNOLOGI MALAYSIA

FLUID DYNAMICS AND THERMODYNAMICS NUMERICAL MODELLING  
OF SELF-HEALING FIBRE REINFORCED LAMINATED COMPOSITES

KAM CHEE ZHOU

A thesis submitted in fulfilment of the  
requirements for the award of the degree of  
Doctor of Philosophy (Civil Engineering)

Faculty of Civil Engineering  
Universiti Teknologi Malaysia

MARCH 2018

*To my family*

## **ACKNOWLEDGEMENT**

First and foremost, I would like to express my sincere appreciation to the supervisor of present study, Dr Ahmad Kueh Beng Hong for his continual dedicated guidance, professional advices, encouragement, support and motivation in effort to complete this research.

Apart from this, I would like to extend my gratitude and appreciation to all the researchers from the Construction Research Centre, Faculty of Civil Engineering, Universiti Teknologi Malaysia, who had been very helpful and patient in providing assistance throughout the work.

Also, I would like to extend my special thanks to my colleagues and friends for their friendship, continuous support, understanding, as well as encouragement. Moreover, I would like to express my gratitude to Universiti Teknologi Malaysia for the facilities and opportunities given for me to pursue this study.

Last but not least, I would like to thank my family for their patience, prayers, undivided support and encouragement to me during this study.

## ABSTRACT

Inspired by the bleeding mechanism in living organisms to heal injury for survival, such capability has been integrated into a damaged laminate composite for autonomous internal repairing to extend its service life. The main healing mechanisms include infiltration of healing liquid into the crack plane, resulted from the breaching of pre-embedded vessels, which is triggered by a damage event. The later polymerization of the healant serves to restore the strength of the crack plane and hence inhibits further crack growth. The best healing performance is generally governed by both infiltration and polymerization rates of healing liquid at the crack tip. In ensuring assessment of these rates without excessive computational burden but free from the companion numerical stability-consistency-accuracy issues, in-house hydrodynamic and thermodynamic models based on the weak form Galerkin finite element (FE) method have been developed in this study. To simulate the micro-scale isothermal hydrodynamics of the Newtonian liquid, one-dimensional (1D) incompressible Stokes equations have been solved using the penalty function method. Computational matters, such as the feasible penalty parameter ( $\gamma_p$ ) for multiple flow geometries of single straight micro-channel, are discussed and numerically addressed. Meanwhile, the polymerization mechanics of healing liquid in a straight crack channel is obtained by solving the heat conduction formulation coupled with the phenomenological Arrhenius's rate equation and Crank-Nicolson time scheme. It is observed that the iterative Uzawa's technique, which employs forcing term correction in terms of the previous velocity solution, coupled with another forcing term correction in terms of the previous divergence of velocity solution is capable of eliminating the instability of axial pressure distribution and inconsistency of the conventional penalty model setting. Additionally, implementing termination criterion by equalizing the order of both maximum elemental divergence of velocity ( $EDV_{\max}$ ) and penalty parameter ensures stability, consistency, and accuracy of solution for  $1 \times 10^1 \leq \gamma_p \leq 1 \times 10^{11}$ . Adopting similar termination technique for the Crank-Nicolson predictor-corrector time integration scheme with the penalty formulation, the proposed model is capable of capturing the flow front motion in micro-channel by electing the temporal mesh size ( $\Delta t$ ) from a function of hydraulic diameter ( $D_h$ ) and spatial mesh size ( $\Delta x$ ). Parametric study for temperature and cure degree evolution by varying pre-exponential factor ( $\tilde{A}$ ), activation energy ( $\tilde{E}$ ),  $\tilde{n}$ -th order of reaction, and ultimate enthalpy of cure ( $\tilde{H}$ ) has been performed thoroughly where an optimal coupling between  $\tilde{A}$  and  $\tilde{E}$  is identified as the dominating factor in achieving the most favored repairing behavior. While the order of reaction imparts less significance in the evaluation, it is observed that polymeric healant with a higher numerical value of  $\tilde{H}$  is not beneficial either. The principal contribution of the present study includes the construction of a series of FE Eulerian frameworks that are reliable, without excessive computational burden, in assessing key diffusive mechanistic variables of extrinsic self-healing mechanisms in achieving optimal strength recovery of straight crack geometry in polymeric materials.

## ABSTRAK

Diilhamkan oleh mekanisme pendarahan dalam organisma hidup demi menyembuhkan kecederaan untuk kesinambungan hidup, keupayaan ini telah disepadukan ke dalam komposit lamina yang rosak untuk pembaikan dalaman autonomi demi pemanjangan hayat perkhidmatannya. Mekanisme penyembuhan utama termasuk penyusupan cecair penyembuh ke dalam pelan retak hasil daripada kebocoran saluran pra-tanam, yang dicitus oleh peristiwa kerosakan. Pempolimeran penyembuh seterusnya berfungsi untuk memulihkan kekuatan kawasan retak dan menghalang pertumbuhan retak. Prestasi penyembuhan terbaik biasanya dikawal oleh kedua-dua kadar penyusupan dan pempolimeran cecair penyembuh di hujung retak. Untuk menilai kekadaran ini tanpa beban komputeran yang berlebihan, tetapi bebas daripada masalah sambilan kestabilan-konsistensi-ketepatan, model hidrodinamik dan termodinamik bina-diri berdasarkan kaedah unsur terhingga (FE) Galerkin bentuk lemah telah dibangunkan di dalam kajian ini. Untuk simulasi hidrodinamik cecair Newtonian sesuhu berskala mikro, persamaan Stokes tak mampat satu dimensi (1D) telah diselesaikan dengan kaedah fungsi penalti. Isu komputeran, seperti kesesuaian parameter penalti ( $\gamma_p$ ) dengan pelbagai geometri aliran untuk saluran mikro lurus tunggal, telah dibincang dan ditangani secara berangka. Sementara itu, mekanik pempolimeran cecair penyembuh dalam saluran retak lurus telah diperolehi dengan menyelesaikan formulasi aliran haba yang dipasangkan dengan persamaan kadar fenomenologi Arrhenius dan skim masa Crank-Nicolson. Teknik lelaran Uzawa yang menggunakan pembetulan terma daya dalam bentuk penyelesaian halaju sebelumnya, dipasangkan dengan pembetulan terma daya dalam bentuk perbezaan penyelesaian halaju sebelumnya, telah diperhatikan mampu menghapus ketidakstabilan taburan tekanan paksi dan kekurangan konsistensi oleh ketetapan model penalti konvensional. Selain itu, pelaksanaan kriteria penamatan dengan menyamakan peringkat kedua-dua perbezaan halaju unsur maksimum dan parameter penalti mampu memastikan kestabilan, konsistensi, dan ketepatan penyelesaian untuk  $1 \times 10^1 \leq \gamma_p \leq 1 \times 10^{11}$ . Dengan teknik penamatan yang sama untuk skim integrasi masa peramal-pembetul Crank-Nicolson dengan formulasi penalti, model yang dicadang mampu menentukan pergerakan hadapan aliran dalam saluran-mikro dengan memilih saiz unsur tempoh ( $\Delta t$ ) daripada fungsi diameter hidraulik ( $D_h$ ) dan saiz unsur ruangan ( $\Delta x$ ). Kajian parametrik terhadap evolusi suhu dan tahap pengawetan dengan mengubah faktor pra-eksponen ( $\tilde{A}$ ), tenaga pengaktifan ( $\tilde{E}$ ), tindakbalas peringkat ke- $\tilde{n}$ , dan entalpi muktamad untuk awetan ( $\tilde{H}$ ) telah dijalankan dengan teliti di mana gandingan optima antara  $\tilde{A}$  dan  $\tilde{E}$  telah dikenalpasti sebagai faktor dominasi dalam mencapai kelakuan pembaikan terbaik. Walaupun peringkat reaksi kurang memberi implikasi dalam penilaian, penyembuh polimer dengan nilai  $\tilde{H}$  yang lebih tinggi juga diperhatikan tidak berfaedah. Sumbangan utama daripada kajian ini termasuk binaan satu siri rangka kerja FE Eulerian yang mantap, kurang beban komputeran, dalam menilai pembolehkan mekanistik sebaran utama untuk mekanisme penyembuhan diri ekstrinsik demi mencapai pemulihan kekuatan optima bagi geometri retak lurus bahan polimer.

## TABLE OF CONTENTS

CHAPTER	TITLE	PAGE
	<b>DECLARATION</b>	ii
	<b>DEDICATION</b>	iii
	<b>ACKNOWLEDGEMENT</b>	iv
	<b>ABSTRACT</b>	v
	<b>ABSTRAK</b>	vi
	<b>TABLE OF CONTENTS</b>	vii
	<b>LIST OF TABLES</b>	x
	<b>LIST OF FIGURES</b>	xii
	<b>LIST OF ABBREVIATIONS</b>	xxii
	<b>LIST OF SYMBOLS</b>	xxiv
	<b>LIST OF APPENDICES</b>	xxvi
<b>1</b>	<b>INTRODUCTION</b>	<b>1</b>
	1.1 Background of the Study	1
	1.2 Problem Statement	7
	1.3 Objectives of the Study	8
	1.4 Scopes of the Study	8
	1.5 Significance of the Study	11
	1.6 Outlines of the Thesis	13
<b>2</b>	<b>LITERATURE REVIEW</b>	<b>15</b>
	2.1 External Self-Healing Polymeric Materials	15
	2.2 Motivation towards Numerical Examination on Fluid and Polymerization Mechanics	25
	2.2.1 Fluid Mechanics in Extrinsic Self-healing Polymeric Materials	32
	2.2.2 Polymerization Mechanics in Extrinsic Self-healing Polymeric Materials	36

2.3	Diffusive Characteristic of Fluid Flow and Polymerization in Galerkin FE Set-up	39
2.3.1	Incompressible Flow Model	42
2.3.1.1	Mixed Functional for Incompressible Fluid Flow Model Formulation	43
2.3.1.2	Penalty Functional for Incompressible Fluid Flow Model Formulation	48
2.3.1.3	Iterative Penalty Functional for Incompressible Fluid Flow Model Formulation	53
2.3.1.4	Penalty FE Formulation for Time-dependent Viscous Incompressible Flow	60
2.3.2	Polymerization Model	66
2.3.2.1	Numerical Stability, Consistency, and Accuracy in Polymerization Modeling	70
2.3.2.2	Optimal Cure Chemistry	73
2.4	Summary	79
<b>3</b>	<b>DEVELOPMENT OF IN-HOUSE HYDRODYNAMICS AND THERMODYNAMICS MODELS</b>	<b>82</b>
3.1	Governing Equations of Incompressible Flow Filling	84
3.1.1	Semi-discrete Incompressible Flow Model	98
3.1.2	Full-discrete Incompressible Flow Model	106
3.2	Governing Equations of Heat Transfer Analysis	109
3.2.1	Semi-discrete Heat Transfer Model	111
3.2.2	Full-discrete Heat Transfer Model	114
3.3	Summary	117
<b>4</b>	<b>STABLE AND ACCURATE PRESSURE SOLUTION FOR A STRAIGHT MICRO-CHANNEL</b>	<b>119</b>
4.1	Conventional Penalty Galerkin Finite Element Setting	119



4.2	Iterative Penalty Galerkin Finite Element Setting	131
4.3	Optimal Framework of Iterative Penalty Galerkin Finite Element Setting	142
4.4	Modified Iterative Penalty Galerkin Finite Element Setting	148
4.5	Summary	154
<b>5</b>	<b>MICRO-FLOW FRONT TRACKING BASED ON PENALTY GALERKIN FINITE ELEMENT MODEL</b>	<b>155</b>
5.1	Nature of the Proposed Time-dependent Framework	155
5.2	Optimal Coupling of Spatial Mesh Size and Temporal Mesh Size	167
5.3	Summary	181
<b>6</b>	<b>EXTRINSIC HEAL MODELING OF A STRAIGHT CRACK</b>	<b>183</b>
6.1	Steady Heat Transfer	183
6.2	Transient Heat Transfer	185
6.3	Key Evaluation Criterion on Optimal Mechanical Performance	190
6.4	Optimization Analysis based on Yuan et al. (2009)	193
6.5	Summary	198
<b>7</b>	<b>CONCLUSIONS AND RECOMMENDATIONS</b>	<b>200</b>
7.1	Conclusions	200
7.2	Recommendations	204
	<b>REFERENCES</b>	<b>205</b>
	Appendices A – J	212 – 323

## LIST OF TABLES

TABLE NO.	TITLE	PAGE
2.1	General features of extrinsic and intrinsic-based approaches in self-healing polymeric materials (Zhu et al., 2015).	17
2.2	The main discussions in the literature categorized based on the practical aspect of implementation.	19
3.1	The scopes and relevant details of the numerical framework focused in the present study.	83
4.1	The mesh domains adopted to solve the micro-flow problem in Alharbi et al. (2003).	121
4.2	The solution accuracy of all trial pairs of spatial mesh size and penalty parameter.	141
4.3	The generalized micro-flow test problems for the iterative penalty model.	142
4.4	The suggested values of $\gamma_p$ corresponding to the range of $l/D_h$ .	144
4.5	Micro-flow problems for validation.	145
5.1	Typical analytical solutions for the surface-tension driven micro-flow cases.	168
5.2	The feasible range of temporal mesh size of each micro-flow case.	175
5.3	Influence of parameters based on (a) $\frac{\Delta x}{\Delta t}$ and (b) $\left(\frac{\Delta x}{\Delta t}\right)^2$ .	176
5.4	The temporal mesh size adopted for validation based on the proposed parameter.	178
5.5	The validation of the model in present study to that of analytical solution.	181
6.1	Physical properties of the heat transfer problem in Lewis et al. (2004).	184
6.2	Geometrical details of the heat conduction approximation and the physical properties of polyester (Rouison et al., 2004).	187
6.3	The ultimate enthalpy of cure and the components of the autocatalytic model for polyester (Rouison et al., 2003, 2004).	187

6.4	The couplings of spatial mesh and temporal mesh size in examining numerical stability and accuracy.	188
6.5	The polymerization kinetics and the corresponding strength recovery based on the varying content of the catalyst (Yuan et al., 2009).	190
6.6	The geometry details of the cure domain and physical properties of the self-healing epoxy (Yuan et al., 2009).	191
6.7	The summary on favourable range of key components in $\tilde{n}$ -th order reaction kinetic towards optimal strength recovery.	199
7.1	Summary on guidelines and treatment for solving Stokes equations by adopting penalty set-ups in the present study.	202
7.2	Summary on main components of phenomenological $\tilde{n}$ -th order of reaction kinetic towards optimal strength recovery.	203
G.1	Geometric constant for frictional consideration (White and Corfield, 2006).	288
H.1	5mm/s with length of (a) 1mm (b) 6mm (c) 11mm (d) 16mm and (e) 20mm.	294
H.2	5cm/s with length of (a) 1mm (b) 6mm (c) 11mm (d) 16mm and (e) 20mm.	299
H.3	5m/s with length of (a) 1mm (b) 6mm (c) 11mm (d) 16mm and (e) 20mm.	304
J.1	Typical fluid properties of surface tension flow (Saha and Mitra, 2008).	323

## LIST OF FIGURES

<b>FIGURE NO.</b>	<b>TITLE</b>	<b>PAGE</b>
1.1	Typical (a) crack initiation (Zhang and Li, 2016) and (b) damage modes in polymeric materials (Blaiszik et al., 2010).	2
1.2	Innovative healing concepts corresponding to thermoplastic and thermoset polymers (Meng and Li, 2013; Yang et al., 2015; Patrick et al., 2016).	3
1.3	The conceptual synthetic system as inspired by the biological repairing route (Blaiszik et al., 2010).	4
1.4	Schematic of the (a) microcapsule system (b) typical crack propagation and (c) flow and subsequent solidification of healant in crack geometry (Murphy and Wudl, 2010).	4
1.5	Typical consideration scopes and mechanics in extrinsic self-healing polymeric system.	5
1.6	The domain of (a) presume crack geometry and (b) fluid flow and polymerization.	9
2.1	The key observation on the (a) healing potential and (b) healing speed of the intrinsic and extrinsic-based healing systems (Blaiszik et al., 2010).	16
2.2	Repair large portion damage through vascular healing system (a) schematic representation (Krull et al., 2016) and (b) practical specimen (White et al., 2014).	18
2.3	The key summarizations on the external self-healing polymeric materials (Hillewaere and Du Prez, 2015).	20
2.4	Typical (a) damage modes in polymeric materials and (b) mechanical tests in self-healing polymer literature (Tsangouri et al., 2015).	22
2.5	Schematic representation of the main mechanisms of external self-healing in polymer matrix based on TDCB framework (Jones and Dutta, 2010; Brown et al., 2005).	23
2.6	The main chained kinetics and mechanics relevant to optimal design of external self-healing system.	24

2.7	The (a) FE damage-heal framework in assessing the mechanical and healing kinetics of a typical spring structure and (b) relevant structural performance (Schimmel and Remmers, 2006).	25
2.8	The (a) FE damage-heal framework in assessing the mechanical and healing kinetics of a peel structure and (b) relevant structural performance with and without repairing event (Schimmel and Remmers, 2006).	27
2.9	The (a) illustration of multi-phase framework targeted for self-healing polymer with the resulting (b) damage and (c) healing configurations throughout the numerical analysis (Shojaei et al., 2015).	28
2.10	The 3D FE framework in assessing the mechanical and healing kinetics (a) problem geometry and boundary condition (b) damage (left) and healing (right) evaluation and (c) enlarged view of the numerical examination (Bluhm et al., 2015).	30
2.11	The geometry details and numerical mesh of the compact tension specimen (Alsheghri and Al-Rub, 2016).	30
2.12	The effective load bearing portion of the compact tension specimen (Alsheghri and Al-Rub, 2016).	31
2.13	The von Mises contour of compact tension specimen throughout the numerical assessment (Alsheghri and Al-Rub, 2016).	32
2.14	Self-healing polymeric laminate (Trask et al., 2007) (a) schematic layout and the infiltration response upon impacted and (b) enlarged view of the cross-sectional damage network.	33
2.15	The shear crack (a) infiltration response under the aid of the microscopy (Trask et al., 2007) and (b) numerical set-up for infiltration modeling (Hall et al., 2015).	34
2.16	The numerical assessment of infiltration response in shear crack geometry (Hall et al., 2015) (a) transient progression of the healant with viscosity of 0.05Pa s and (b) fill behavior of healant with different viscosities.	35
2.17	Typical cure examination set-up (a) specimens of dynamic mechanical analysis and (b) oscillatory parallel plate rheometer (Liu et al., 2006, 2009).	36
2.18	The curing details and behavior of DCPD subjected to three different concentrations (Kessler and White, 2002).	37

2.19	The cure behaviors of endo-DCPD upon subjected to the variation of catalyst and cure temperature (Yang and Lee, 2014).	37
2.20	The influence of (a) catalyst content (b) type of catalyst and (c) cure temperature on the cure strength of DCPD (Mauldin et al., 2012).	38
2.21	The cure degree and strength development of DCPD upon subjected to variation of catalysyt concentration and cure temperature (Aldridge et al., 2014).	39
2.22	The use of commercial software in (a) validating numerical flow front to that of experimental and (b) simultaneously assessing velocity, pressure and temperature solutions within the flow domain at different time frame (Wang et al., 2012).	40
2.23	Typical (a) analysis in curing of polymeric materials and (b) numerical assessment of chained dependent variables (Rabearison et al., 2009).	41
2.24	Typical numerical method in solving viscous incompressible flow.	43
2.25	The Patch test results of the common interpolation pairs for (a) a single quadrilateral element and (b) assembly of quadrilateral elements (Zienkiewicz et al., 1986).	46
2.26	Pressure solutions of steady flow through sudden expansion corresponding to typical mixed quadralateral interpolations (Huyakorn et al., 1978).	47
2.27	Velocity contour of flow over a step corresponding to the variation of spatial mesh density (Gresho and Lee, 1981).	48
2.28	The (a) geometry and boundary conditions of non-leaky driven unit cavity and (b) axial velocity as well as pressure solutions at $y = 0.8$ of the driven unit cavity (Carey and McLay, 1986).	49
2.29	The pressure solution corresponding to the family of interpolation as well as mesh density (Carey and McLay, 1986).	50
2.30	The (a) geometry and boundary condition and (b) axial pressure distribution of flow between parallel plates (Chen et al., 1995).	51
2.31	The (a) problem geometry along with boundary conditions and (b) true as well as numerical solution of planar Poiseuille flow (Pelletier et al., 1989).	52

2.32	General procedure of gradient technique in solving mixed-variable system (Zienkiewicz et al., 1985).	53
2.33	The (a) procedures of gradient solver and iterative divergence of velocity (Zienkiewicz et al., 1985) adopting (b) gradient solver and (c) both conventional penalty and gradient solver in solving 2:1 flow contraction problem.	54
2.34	The iterative divergence of velocity field (Zienkiewicz et al., 1985) in (a) single float and (b) double float system.	55
2.35	The (a) mesh of a quadrant of a round pipe (b) the velocity contour and (c) the pressure contour (Reddy et al., 1992).	56
2.36	The radial velocity solutions corresponding to the value of penalty parameter in typical gradient solvers (Reddy et al., 1992).	57
2.37	The geometry along with boundary conditions and typical mesh for 1:2 expansion flow problem (Reddy et al., 1993).	57
2.38	The (a) percentage of error of the iterative solvers and (b) accuracy plot for the coupling of spatial mesh size and convergence tolerance (Reddy et al., 1993).	58
2.39	The (a) percentage of error and (b) accuracy plot for the coupling of penalty parameter and convergence tolerance (Reddy et al., 1993).	59
2.40	The mesh and boundary details along with the dynamic velocity contours for fluid flow past a square step (Bercovier and Engelman, 1979).	61
2.41	Typical procedures for the predictor-corrector time integration scheme by Engelman (1982).	62
2.42	Typical procedures for the predictor-corrector time integration scheme by Hughes et al. (1979).	62
2.43	The (a) transient Stokes approximation for Couette flow and (b) transient Navier-Stokes approximation for flow over square step (Hughes et al., 1979).	64
2.44	Typical procedures for the velocity-explicit/pressure-implicit time integration scheme (Mizukami, 1985).	65
2.45	The (a) mesh and boundary condition for step flow and the effect of varying temporal mesh size and penalty parameter on the (b) stability behavior and (c) convergence behavior (Mizukami, 1985).	66

2.46	The (a) temperature and (b) cure degree progression following the adoption of numerous temporal mesh sizes (Yi et al., 1997).	67
2.47	The 2D and 3D cure modeling with respective functions of interpolation (Park and Lee, 2001; Park et al., 2003).	67
2.48	The validated 1D and 3D numerical performance to that of experimental framework (Behzad and Sain, 2007).	68
2.49	Typical (a) mesh domain and (b) temperature and cure contour for 3D cure modeling (Behzad and Sain, 2007).	69
2.50	The truncation error coefficients corresponding to the variation of $\frac{\Delta t}{(\Delta x)^2}$ (Yang and Gu, 2006).	71
2.51	The accuracy of various spatial mesh size under the variation of $\frac{\Delta t}{(\Delta x)^2}$ (Yang and Gu, 2006).	72
2.52	Typical lap shear strength corresponding to numerous epoxy blends (Everitt et al., 2015).	74
2.53	The correspondence of self healing efficiency in width-tapered double cantilever beam set-up to bonded surface area (Ghazali et al., 2016).	75
2.54	The (a) parametric variables in cure cycle (b) cure response corresponding to the variation of ramp rate and dwell temperature and (c) examination on the cure responses under exhaustive trials and genetic cure cycle profiles (Struzziero and Skordos, 2017).	76
2.55	The (a) key criteria in achieving good polymeric composite curing (b) key components in genetic algorithm framework and (c) fitness function examination with and without curing stress constraint (Ruiz and Trochu, 2005, 2006).	79
3.1	The (a) presumed crack geometry and modeled domains of (b) fluid flow as well as (c) polymerization process in the present study.	83
3.2	Mass fluxes across a differential control volume (Fox et al., 2004).	85
3.3	Momentum fluxes across a differential control volume (Fox et al., 2004).	87
3.4	Stresses acting on a differential control volume along (a) $x$ - $y$ plane (b) $y$ - $z$ plane and (c) $z$ - $x$ plane (Fox et al., 2004).	90
3.5	The channel flow with (a) zero relative velocity at solid surfaces and (b) uniform flow at a given cross section (Fox et al., 2004).	97



3.6	The local and global approximation of the velocity and pressure variables.	104
3.7	The solution procedure of the penalty algorithm.	104
3.8	Iterative loops for transient solutions.	109
3.9	Heat fluxes across a differential control volume.	109
3.10	The local and global approximations of the temperature variable.	113
3.11	The solution procedures for steady heat transfer analysis with constant heat generation source.	114
3.12	The solution procedure of the heat conductive polymerization model.	116
3.13	The expected progressive (a) filled length and (b) axial pressure distribution by means of the framework presented in Section 3.1.2.	117
3.14	The expected progressive (a) temperature and (b) cure fraction evolution by means of the framework presented in Section 3.2.2.	118
4.1	The (a) geometry and (b) the corresponding axial pressure distribution of micro-scale straight array in Alharbi et al. (2003).	120
4.2	Inlet pressure of different mesh domains under the variation of penalty parameter.	122
4.3	Axial pressure distribution for various mesh domains under the variation of penalty parameter (a) $\gamma_p = 1 \times 10^{10}$ (b) $\gamma_p = 1 \times 10^{11}$ (c) $\gamma_p = 1 \times 10^{12}$ (d) $\gamma_p = 1 \times 10^{13}$ (e) $\gamma_p = 1 \times 10^{14}$ (f) $\gamma_p = 1 \times 10^{15}$ (g) $\gamma_p = 1 \times 10^{16}$ and (h) $\gamma_p = 1 \times 10^{17}$ .	130
4.4	Plot of the maximum value and the summation of the EDV as well as inlet pressure of 30 iterations for $\gamma_p = 1 \times 10^{13}$ with (a) $h = 100$ (b) $h = 200$ (c) $h = 400$ (d) $h = 800$ (e) $h = 1600$ (f) $h = 3200$ and (g) $h = 6400$ .	132
4.5	Iterative axial pressure distribution of $\gamma_p = 1 \times 10^{13}$ for (a) $h = 100$ (b) $h = 200$ (c) $h = 400$ (d) $h = 800$ (e) $h = 1600$ (f) $h = 3200$ and (g) $h = 6400$ .	139
4.6	Inlet pressure of different meshes under the variation of penalty parameter using the iterative penalty model.	140
4.7	The range of ideal penalty parameter corresponding to micro-flow problems in Table 4.3 for three different inlet velocities.	143
4.8	The ideal range of $\gamma_p$ corresponding to $l/D_h$ .	144

4.9	The validation tests on the proposed framework of the penalty FE model (a) Case A (b) Case B (c) Case C and (d) Case D .	145
4.10	Plots of maximum value of EDV and inlet pressure for $\gamma_p = 1 \times 10^{11}$ and $\gamma_p = 1 \times 10^{12}$ , which correspond to (a) Case A (b) Case B (c) Case C and (d) Case D.	146
4.11	The EDV of all validation cases from conventional set-up with $\gamma_p = 1 \times 10^{11}$ and $\gamma_p = 1 \times 10^{12}$ .	148
4.12	The progressing trend between EDV and $P_{in}$ for (a) $\gamma_p = 1 \times 10^1$ (b) $\gamma_p = 1 \times 10^2$ (c) $\gamma_p = 1 \times 10^3$ (d) $\gamma_p = 1 \times 10^4$ (e) $\gamma_p = 1 \times 10^5$ (f) $\gamma_p = 1 \times 10^6$ (g) $\gamma_p = 1 \times 10^7$ (h) $\gamma_p = 1 \times 10^8$ (i) $\gamma_p = 1 \times 10^9$ (j) $\gamma_p = 1 \times 10^{10}$ (k) $\gamma_p = 1 \times 10^{11}$ and (l) $\gamma_p = 1 \times 10^{12}$ .	152
4.13	Axial pressure distribution for (a) $\gamma_p = 1 \times 10^1$ (b) $\gamma_p = 1 \times 10^2$ (c) $\gamma_p = 1 \times 10^3$ (d) $\gamma_p = 1 \times 10^4$ (e) $\gamma_p = 1 \times 10^5$ (f) $\gamma_p = 1 \times 10^6$ (g) $\gamma_p = 1 \times 10^7$ (h) $\gamma_p = 1 \times 10^8$ (i) $\gamma_p = 1 \times 10^9$ (j) $\gamma_p = 1 \times 10^{10}$ (k) $\gamma_p = 1 \times 10^{11}$ and (l) $\gamma_p = 1 \times 10^{12}$ .	153
5.1	The transient axial pressure distribution for $\gamma_p = 1 \times 10^1$ under the variation of temporal mesh size.	156
5.2	The transient axial pressure distribution under the variation of both temporal mesh size and penalty parameter (a) $\gamma_p = 1 \times 10^2$ (b) $\gamma_p = 1 \times 10^3$ and (c) $\gamma_p = 1 \times 10^4$ .	158
5.3	The transient axial pressure distributions for (a) $\gamma_p = 1 \times 10^5$ (b) $\gamma_p = 1 \times 10^6$ (c) $\gamma_p = 1 \times 10^7$ and (d) $\gamma_p = 1 \times 10^8$ .	161
5.4	The transient axial pressure distribution under the variation of both temporal mesh size and penalty parameter (a) $\gamma_p = 1 \times 10^9$ (b) $\gamma_p = 1 \times 10^{10}$ (c) $\gamma_p = 1 \times 10^{11}$ and (d) $\gamma_p = 1 \times 10^{12}$ .	163
5.5	The progression of inlet pressure following the variation of both temporal mesh size and penalty parameter (a) $\gamma_p = 1 \times 10^1$ (b) $\gamma_p = 1 \times 10^2$ (c) $\gamma_p = 1 \times 10^3$ (d) $\gamma_p = 1 \times 10^4$ (e) $\gamma_p = 1 \times 10^5$ (f) $\gamma_p = 1 \times 10^6$ (g) $\gamma_p = 1 \times 10^7$ (h) $\gamma_p = 1 \times 10^8$ (i) $\gamma_p = 1 \times 10^9$ (j) $\gamma_p = 1 \times 10^{10}$ (k) $\gamma_p = 1 \times 10^{11}$ and (l) $\gamma_p = 1 \times 10^{12}$ .	166
5.6	The flow front for surface-tension flow in $20\mu\text{m}$ square micro-channel.	168
5.7	Engineering-based procedure in the search of underlying parameter.	169

5.8	Inlet pressure solution (left) and its enlarged view (right) of the end filling of $20\mu\text{m}$ square micro-channel with length of (a) 2mm (b) 4mm (c) 6mm (d) 8mm and (e) 10mm under different temporal mesh sizes.	171
5.9	Inlet pressure solution (left) and its enlarged view (right) of the end filling of $60\mu\text{m}$ square micro-channel with length of (a) 2mm (b) 4mm (c) 6mm (d) 8mm and (e) 10mm under different temporal mesh sizes.	172
5.10	Inlet pressure solution (left) and its enlarged view (right) of the end filling of $100\mu\text{m}$ square micro-channel with length of (a) 2mm (b) 4mm (c) 6mm (d) 8mm and (e) 10mm under different temporal mesh sizes.	173
5.11	The (a) minimum and (b) maximum range of the feasible temporal mesh size of each cross-section following the channel length increment.	174
5.12	The variation of the parameter (a) $\frac{\Delta x}{\Delta t}$ (b) $(\frac{\Delta x}{\Delta t})^2$ (c) $D_h \frac{\Delta x}{\Delta t}$ (d) $D_h (\frac{\Delta x}{\Delta t})^2$ (e) $v_{in} D_h \frac{\Delta x}{\Delta t}$ and (f) $v_{in} D_h (\frac{\Delta x}{\Delta t})^2$ corresponding to Reynolds number.	177
5.13	The infilling length (left) and axial pressure distribution (right) for $20\mu\text{m}$ squared section with flow length of (a) 2mm (b) 4mm (c) 6mm (d) 8mm and (e) 10mm.	180
6.1	Heat conduction analysis with constant heat generation term (Lewis et al., 2004).	184
6.2	Validation of the source code with axial temperature distribution of Lewis et al. (2004).	185
6.3	The (a) experimental set-up and (b) dynamic temperature profile of the polyester curing in Rouison et al. (2004).	186
6.4	The dynamic temperature profiles corresponding to the couplings of different spatial and temporal mesh sizes (a) $h = 2$ (b) $h = 4$ (c) $h = 8$ (d) $h = 16$ (e) $h = 32$ and (f) $h = 64$ .	189
6.5	The cure progression of different sets of polymerization kinetics.	192
6.6	The cure temperature profile of different sets of polymerization kinetics.	192
6.7	The cure ratio corresponding to the variation of the polymerization kinetics.	194
6.8	The peak cure temperature corresponding to the variation of the polymerization kinetics.	196

6.9	The optimal ratio corresponding to the variation of the polymerization kinetics.	197
A.1	The source code for the conventional penalty Galerkin FE model.	214
A.2	The source code for (a) iterative solution of velocity and pressure variables (b) iterative $EDV_{\max}$ as well as $EDV_{\text{sum}}$ and (c) post-computation.	217
A.3	The source code for the iterative solution of velocity and pressure variables in modified setting.	218
B.1	The source code for the transient penalty Galerkin finite element model (cont)	219
B.2	The source code for the transient penalty Galerkin finite element model.	222
C.1	The source code employed to compute steady temperature profile due to heat generation source.	224
D.1	The source code for the transient heat conductive polymerization analysis (cont)	225
D.2	The source code for the transient heat conductive polymerization analysis.	228
E.1	Plot of the maximum value and the summation of EDV as well as inlet pressure of 30 iterations for $\gamma_p = 1 \times 10^{10}$ with (a) $h = 100$ (b) $h = 200$ (c) $h = 400$ (d) $h = 800$ (e) $h = 1600$ (f) $h = 3200$ and (g) $h = 6400$ .	230
E.2	Plot of the maximum value and the summation of EDV as well as inlet pressure of 30 iterations for $\gamma_p = 1 \times 10^{11}$ with (a) $h = 100$ (b) $h = 200$ (c) $h = 400$ (d) $h = 800$ (e) $h = 1600$ (f) $h = 3200$ and (g) $h = 6400$ .	231
E.3	Plot of the maximum value and the summation of EDV as well as inlet pressure of 30 iterations for $\gamma_p = 1 \times 10^{12}$ with (a) $h = 100$ (b) $h = 200$ (c) $h = 400$ (d) $h = 800$ (e) $h = 1600$ (f) $h = 3200$ and (g) $h = 6400$ .	232
E.4	Plot of the maximum value and the summation of EDV as well as inlet pressure of 30 iterations for $\gamma_p = 1 \times 10^{14}$ with (a) $h = 100$ (b) $h = 200$ (c) $h = 400$ (d) $h = 800$ (e) $h = 1600$ (f) $h = 3200$ and (g) $h = 6400$ .	233
E.5	Plot of the maximum value and the summation of EDV as well as inlet pressure of 30 iterations for $\gamma_p = 1 \times 10^{15}$ with (a) $h = 100$ (b) $h = 200$ (c) $h = 400$ (d) $h = 800$ (e) $h = 1600$ (f) $h = 3200$ and (g) $h = 6400$ .	234

E.6	Plot of the maximum value and the summation of EDV as well as inlet pressure of 30 iterations for $\gamma_p = 1 \times 10^{16}$ with (a) $h = 100$ (b) $h = 200$ (c) $h = 400$ (d) $h = 800$ (e) $h = 1600$ (f) $h = 3200$ and (g) $h = 6400$ .	235
E.7	Plot of the maximum value and the summation of EDV as well as inlet pressure of 30 iterations for $\gamma_p = 1 \times 10^{17}$ with (a) $h = 100$ (b) $h = 200$ (c) $h = 400$ (d) $h = 800$ (e) $h = 1600$ (f) $h = 3200$ and (g) $h = 6400$ .	236
F.1	The iterative axial pressure distribution of $\gamma_p = 1 \times 10^{10}$ with spatial meshes of (a) 100 (b) 200 (c) 400 (d) 800 (e) 1600 (f) 3200 and (g) 6400 elements.	244
F.2	The iterative axial pressure distribution of $\gamma_p = 1 \times 10^{11}$ with spatial meshes of (a) 100 (b) 200 (c) 400 (d) 800 (e) 1600 (f) 3200 and (g) 6400 elements.	251
F.3	The iterative axial pressure distribution of $\gamma_p = 1 \times 10^{12}$ with spatial meshes of (a) 100 (b) 200 (c) 400 (d) 800 (e) 1600 (f) 3200 and (g) 6400 elements.	258
F.4	The iterative axial pressure distribution of $\gamma_p = 1 \times 10^{14}$ with spatial meshes of (a) 100 (b) 200 (c) 400 (d) 800 (e) 1600 (f) 3200 and (g) 6400 elements.	265
F.5	The iterative axial pressure distribution of $\gamma_p = 1 \times 10^{15}$ with spatial meshes of (a) 100 (b) 200 (c) 400 (d) 800 (e) 1600 (f) 3200 and (g) 6400 elements.	272
F.6	The iterative axial pressure distribution of $\gamma_p = 1 \times 10^{16}$ with spatial meshes of (a) 100 (b) 200 (c) 400 (d) 800 (e) 1600 (f) 3200 and (g) 6400 elements.	279
F.7	The iterative axial pressure distribution of $\gamma_p = 1 \times 10^{17}$ with spatial meshes of (a) 100 (b) 200 (c) 400 (d) 800 (e) 1600 (f) 3200 and (g) 6400 elements.	286
H.1	Optimal penalty parameter corresponding to inlet pressure solution for (a) $v_{in} = 5\text{mm/s}$ (b) $v_{in} = 5\text{cm/s}$ and (c) $v_{in} = 5\text{m/s}$ .	305
I.1	Iterative elemental divergence of velocity for (a) Case A (b) Case B (c) Case C and (d) Case D.	322
J.1	The axial pressure distribution for flow length of 2mm with $20\mu\text{m}$ cross section.	326

## LIST OF ABBREVIATIONS

CG	–	Conjugate gradient
$CRE_t$	–	Change rate of energy with respect to time
$CRM_t$	–	Change rate of mass with respect to time
$CRMM_t$	–	Change rate of momentum with respect to time
CS	–	Control surface
CV	–	Control volume
DCB	–	Double cantilever beam
DCPD	–	Dicyclopentadiene
DD	–	Discrete divergence
DOF	–	Degree of freedom
EDV	–	Elemental divergence of velocity
$EDV_{max}$	–	Maximum elemental divergence of velocity
$EDV_{sum}$	–	Summation of elemental divergence of velocity
$EF_i$	–	External forces, $i = x, y, z$
ENB	–	Ethylidene-norbornene-based
FE	–	Finite element
GMRES	–	Generalized minimum residual
LBB	–	Ladyzhenskaya-Babuška-Brezzi
MR	–	Minimum residual
$NHF_i$	–	Net heat fluxes, $i = x, y, z$
$NMF_i$	–	Net mass fluxes, $i = x, y, z$
$NMMF_i$	–	Net momentum fluxes, $i = x, y, z$
$NRTE_i$	–	Net release of thermal energy, $i = x, y, z$
PE	–	Percentage of error
SD	–	Steepest descent
SPH	–	Smoothed particle hydrodynamics
PT	–	Progression time
TDCB	–	Tapered double cantilever beam

TEC	–	Truncation error coefficient
TEF <sub><i>i</i></sub>	–	Total external forces, $i = x, y, z$
TFT	–	Total filling time
TNMMF <sub><i>i</i></sub>	–	Total net momentum fluxes, $i = x, y, z$
1D, 2D, 3D	–	One-dimensional, two-dimensional, three-dimensional

## LIST OF SYMBOLS

$a$	–	Acceleration
$A$	–	Area
$\tilde{A}$	–	Pre-exponential factor
$c_a$	–	Acceleration parameter
$c_p$	–	Specific heat capacity
$C$	–	Convective transport matrix
$\hat{C}, \tilde{C}$	–	Proportionality constant
$D$	–	Channel diameter
$D_h$	–	Hydraulic diameter
$e$	–	Sequence number of elemental setting
$\hat{e}_x, \hat{e}_y, \hat{e}_z,$	–	Unit vectors
$\tilde{E}$	–	Activation energy
$f_x, f_y, F, F^*$	–	Force components
$g_x, g_y, g_z$	–	Gravitational components
$\tilde{G}$	–	Heat generation source
$h$	–	Number of spatial mesh size
$\tilde{H}$	–	Ultimate enthalpy of cure
$k_x, k_y, k_z$	–	Thermal conductivity
$\tilde{k}$	–	Reaction rate
$\hat{K}, K^*$	–	Fluid conductance matrix
$K_p$	–	Penalty matrix
$\tilde{K}$	–	Heat conductance matrix
$l, L$	–	Length
$\hat{M}, \tilde{M}$	–	Mass matrix
$M_p$	–	Consistent penalty matrix
$n$	–	Sequence number of iterative step
$\tilde{n}$	–	Order of cure reaction
$\hat{n}_x, \hat{n}_y, \hat{n}_z$	–	Unit normal vectors



$\hat{p}_e$	–	Elemental pressure correction
$P$	–	Pressure
$\hat{P}$	–	Global pressure correction
$q$	–	Elemental heat source
$Q$	–	Total heat transfer
$\hat{Q}$	–	Fluid diffusion matrix
$\tilde{Q}$	–	Heat generation matrix
$r$	–	Ramp rate
$R$	–	Universal gas constant
$Re$	–	Reynolds number
$t$	–	Time
$T$	–	Temperature
$u, v, \vec{v}, U, \hat{U}$	–	Velocity components
$\tilde{v}$	–	Predicted velocity
$V$	–	Volume
$w, w_h, w_p$	–	Weight functions
$\alpha$	–	Cure degree
$\Delta t$	–	Temporal mesh size
$\Delta x$	–	Spatial mesh size
$\Delta y, \Delta z$	–	Directional distance
$\epsilon$	–	Residual norm
$\gamma_p$	–	Penalty parameter
$\mu$	–	Viscosity
$\Omega$	–	Domain boundary
$\Phi, \phi$	–	Shape function
$\Psi, \psi$	–	Shape function
$\rho$	–	Density
$\sigma_{ij}$	–	Normal stress components, $i, j = x, y, z$
$\tau_{ij}$	–	Shear stress components, $i, j = x, y, z$
$\theta$	–	Order of generalized trapezoidal rule
$\Upsilon, v$	–	Shape function

## LIST OF APPENDICES

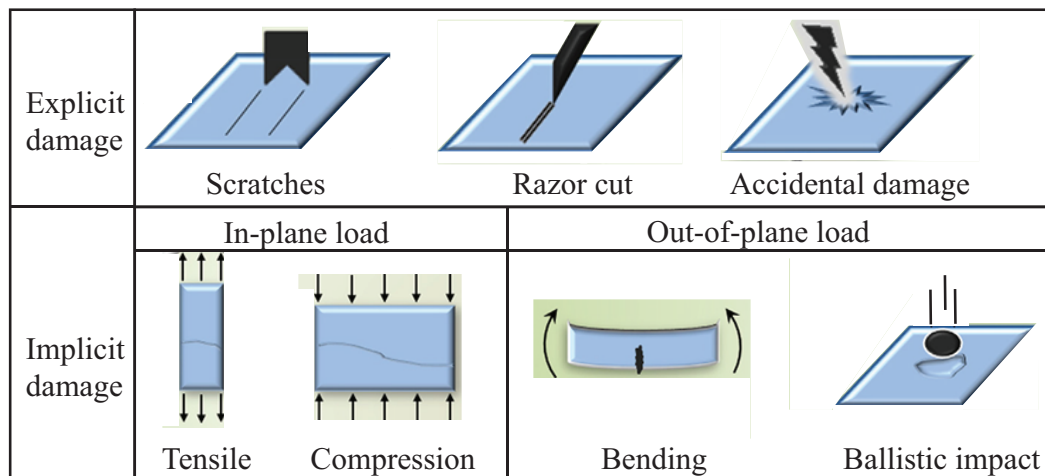
APPENDIX	TITLE	PAGE
A	Source Codes for Steady Incompressible Flow	212
B	Source Code for Transient Incompressible Flow	219
C	Source Code for Heat Transfer Analysis with Heat Generation Source	223
D	Source Code for Transient Heat Transfer Analysis Coupled to Polymerization Kinetics	225
E	The Correspondence of Inlet Pressure Solution to Iterative $EDV_{\max}$ and $EDV_{\text{sum}}$	229
F	Iterative Axial Pressure Distribution	237
G	Analytical Pressure Solution of Viscous Incompressible Flow in A Duct	287
H	The Beneficial Summary of the Numerical Pressure Solutions	289
I	Iterative Divergence of Velocity for Cases A-D	306
J	Analytical Solution for Surface Tension Driven Flow in A Micro-channel	323

# CHAPTER 1

## INTRODUCTION

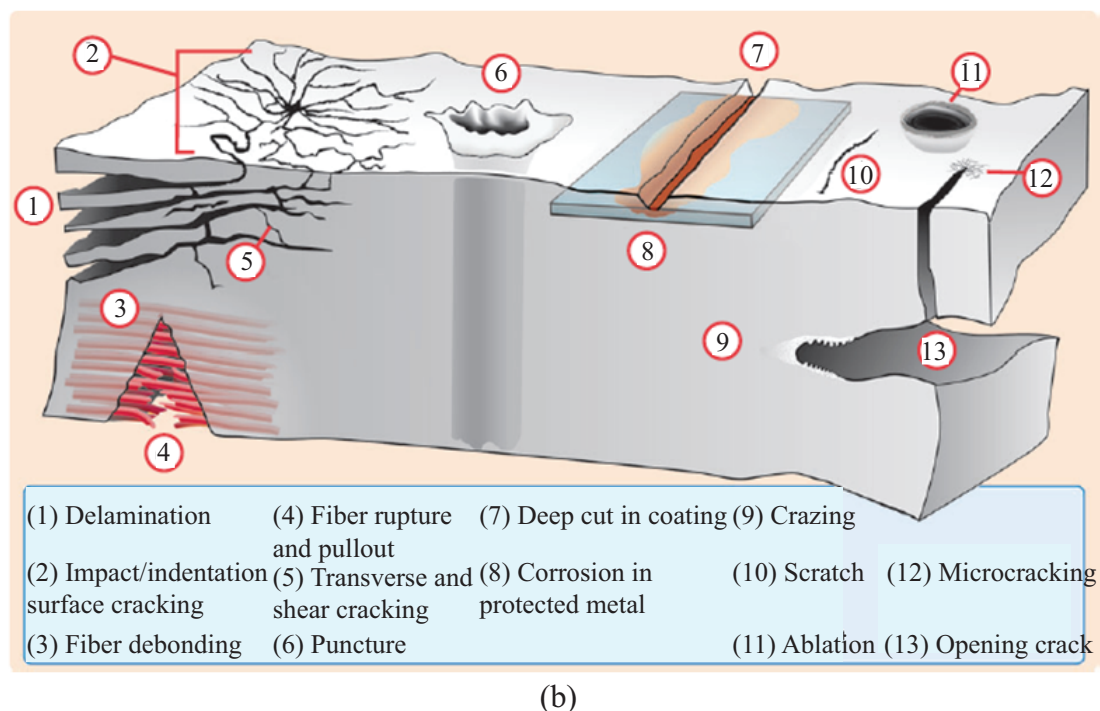
### 1.1 Background of the Study

Despite impressive functionality of polymeric materials in various engineering applications, from thin film to protective coat to fiber reinforced laminae to laminated composite, the material is vulnerable to numerous damage mechanisms (defined either as explicit or implicit damage) as schematically illustrated in Figure 1.1 (a). Typical implicit damage forms as depicted in Figure 1.1 (b) often induce the concerns of structural integrity (Zhang and Rong, 2011; Binder, 2013; Li and Meng, 2015) such as the transverse cracks and delamination that cross and lie between the plies of laminae, respectively. Of more relevance, the polymeric structures in structural application could lose partially the load carrying capability when subjected to these damage events that eventually cause catastrophic failure or fatigue once the cumulative damage intensity and/or severity exceeds the critical threshold.



(a)

**Figure 1.1:** Typical (a) crack initiation (Zhang and Li, 2016) and (b) damage modes in polymeric materials (Blaiszik et al., 2010) (cont)



(b)

**Figure 1.1:** Typical (a) crack initiation (Zhang and Li, 2016) and (b) damage modes in polymeric materials (Blaiszik et al., 2010).

To counteract the degradation of the structural functionality of the material upon damage, the repairing measure shall initiate as early as possible to prohibit the increment of the level of severity. The complexity and hence efficiency of the maintenance scheme is often directly proportional to the intensity as well as severity of the damage events. Despite such awareness, the idea is often less likely implemented due to the difficulty in detecting these barely visible implicit damages. The detecting issue along with the tedious and costly outside-to-inside scratch repair works have motivated various innovative healing routes (Figure 1.2) for the polymeric materials. In general, the intrinsic/internal healing concept is applicable to the thermoplastic polymer due to its reversible switch of the broken crosslinking when subjected to certain stimulus. The extrinsic/external healing concept that generates a new volume of crosslinking is mostly characterized for the thermoset polymer due to its non-reversible network. Note that the implementation route and healing scale vary according to the repairing type achieved by the polymeric crosslinking (Zhang and Rong, 2011; Binder, 2013; Li and Meng, 2015). General details relevant to thermoplastic and thermoset polymeric materials have been highlighted with red and yellow color, respectively.

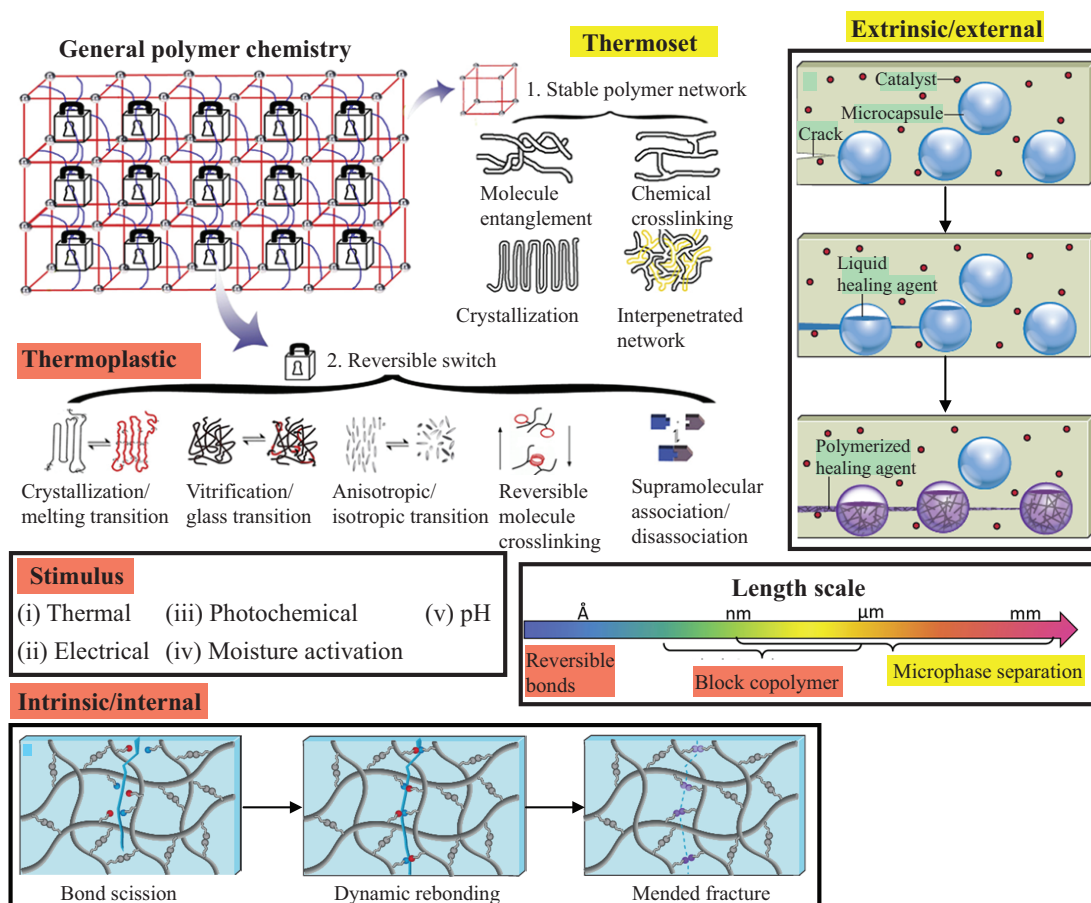


**Figure 1.2:** Innovative healing concepts corresponding to thermoplastic and thermoset polymers (Meng and Li, 2013; Yang et al., 2015; Patrick et al., 2016).

White et al. (2001) demonstrated the autonomous healing of the micro-scale damage in bulk polymer matrix by mimicking the simplified biological self-healing system as given in Figure 1.3. By autonomous, the system is meant to work without any human intervention. The trigger, either damage or wound in respective route, is responsible to initiate the transportation of the healant to the intended destination (e.g. blood delivery for the biological route). The subsequent response, mainly based on the chemical nature, is responsible for the repair of the damage/wound. Despite mimicking, the duration for the healing in synthetic system is much shorter than the biological system.

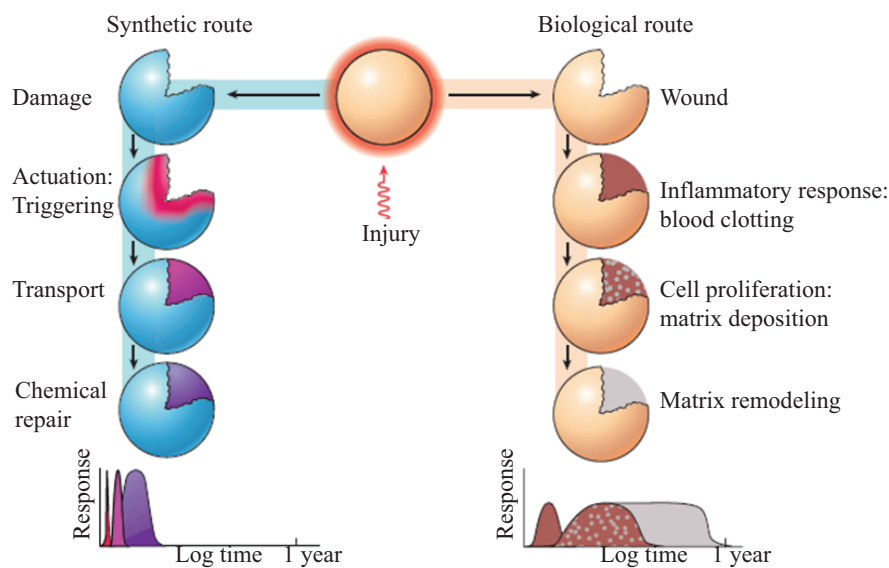


**Figure 1.3:** The conceptual synthetic system as inspired by the biological repairing route (Blaiszik et al., 2010).

The general key mechanisms of the external self-healing system by White et al. (2001) include the rupture of the container (i.e. encapsulated dicyclopentadiene and Grubb's catalyst) that triggers the flow and subsequent solidification of the healing chemical within the damage geometry (refer Figure 1.4 (b-c)) embedded in the bulk epoxy matrix. The term external is used since there is an embedment of an extra healing chemical-filled containers to the host material (Zwaag, 2007; Ghosh, 2009) to perform the autonomous healing functionality once it is damaged. The healing is mechanically triggered by the extending micro-crack that ruptures the embedded containers of the system, thereby attributing to the autonomous characteristic of the synthetic system.

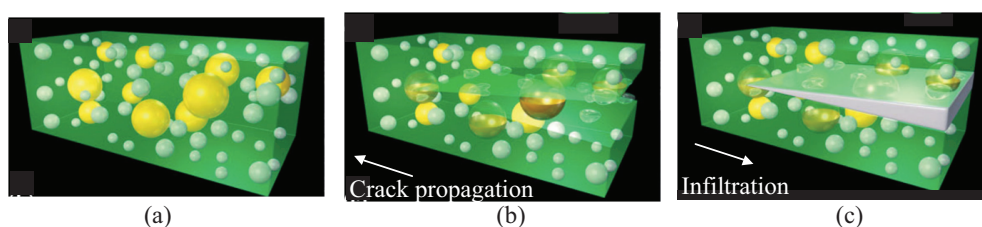


**Figure 1.4:** Schematic of the (a) microcapsule system (b) typical crack propagation and (c) flow and subsequent solidification of healant in crack geometry (Murphy and Wudl, 2010).

The trigger, transport, and chemical repair in the practice of the external self-healing in polymeric materials are generally governed by solid, fluid, and polymerization mechanics along with multiple linear and/or nonlinear constitutive laws as proposed in the current thesis and presented in Figure 1.5. For optimal performance in healing, Zone III is the most desired but of the greatest complexity. This is because it overlaps all three chief mechanics (solid fracture, fluid, and polymerization), and therefore, the most realistic characterization of the healing behavior. When considered separately in a single field fashion (single perspective: Zones I-1, I-2, and I-3), optimality in healing is the lowest although they are of the least complexity in design. An intermediate level of optimality in design can be achieved by overlapping in consideration two of the three main mechanics as illustrated by the II-1, II-2, and II-3 Zones.

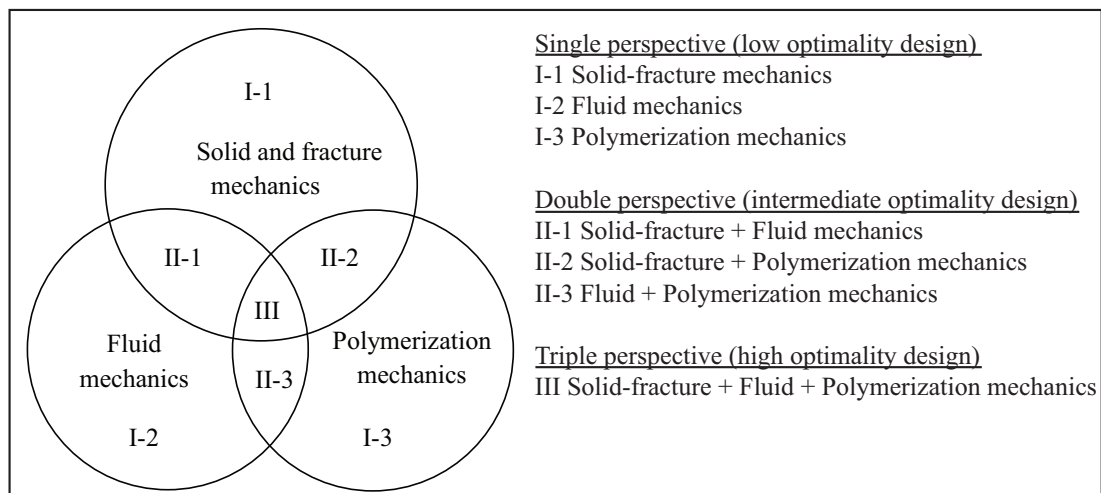


**Figure 1.5:** Typical consideration scopes and mechanics in extrinsic self-healing polymeric system.

For instance, there is no limitation on the incremental size of the containers within Zone I-2 consideration in order to maximize the pumping power on the healing liquid for the infiltration purpose. However, the container size is subjected to constraint if the consideration is arisen from Zone II-1. This is to align with the minimal detrimental loss strength of the specimen due to the containers embedment that is arisen from the consideration in Zone I-1. Various external self-healing trials have since been reported for different polymer matrices as well as their laminates (Hillewaere and Du Prez, 2015), adopting different containers (i.e. microcapsule, hollow fiber, vascular) and healing chemicals (mostly polymeric liquid), aiming at repairing different modes of micro-scale damage. The common goal of these works

remains in the search for the optimized synthetic system of the aforementioned variables in prolonging the service life of the man-made polymeric structures, preferably without human intervention.

Assessment on the optimality of the mechanical performance of the specimen due to the embedment of external healing system, through initial damage loss and final heal recovery of specific variables, is readily achievable based on the solid-fracture mechanics (Zwaag, 2007; Ghosh, 2009; Zhang and Rong, 2011). Nevertheless, a core attention on the fluid flow and polymerization realms of this new evolving scientific practice remains lacking and hence worth to be further addressed. Specifically, the behavior arisen based on the fluid-polymerization mechanics needs to be attached to the much conventional solid-fracture-solid framework to enable a much in-depth mechanical assessment. Note that the extrinsic healing mechanisms itself is of both multi-physics (i.e. structural, fracture, fluid, polymerization, heat transfer) and multi-scales (i.e. micro-crack and macro-specimen) nature. Hence, neglecting fluid flow and polymerization perspective in assessment is less realistic while also preventing the healing performance to achieve to its full potential as readily presented and discussed in Figure 1.5.

Experimental evaluation of both fluid and polymerization mechanics poses considerable difficulty in execution since these events occur within a micro-scale crack domain that is often embedded in the macro-scale opaque geometry. Also, there is a need for a high-end equipment set to capture the effective capturing of the relevant details (e.g. physical, chemical and thermal) that are multi-dimensional spanning as well as highly dynamic for a lengthy period. Numerical evaluation of these mechanics, for instance, based on the finite element (FE) spatial discretization and finite difference temporal discretization, seems practically attractive since a much convenient construction of the virtual environment to that of experimental is possible to deal with the dynamic phenomenon with multi-physics, multi-scales, and multi-dimensional nature.

Nevertheless, the adoption of these popular numerical approaches in evaluating the fluid flow and polymerization behaviors often induces concerns in terms of the numerical stability, consistency, and accuracy (Bathe, 1996; Reddy and Gartling, 2010; Zienkiewicz et al., 2013, 2014). As a matter of fact, the feasibility of the approach as an alternative to that of experimental is generally dependent on the numerical performance generated from the virtual framework constructed. The added advantage of the numerical assessment compared to the experimental framework, if numerous



parametric studies are to be performed on the search of the optimal external healing system, includes the labour-cost-time saving. Yet, it is less persuasive if the employed numerical framework lacks of stability, consistency, and accuracy. Hence, the in-depth discussion on the framework of numerical assessing these extrinsic self-healing mechanism is vital and of great potential to constitute one of the main research streams within the realm of self-healing man-made polymeric materials.

## 1.2 Problem Statement

The virtual framework, self-developed rather than relying on adjusting the features in any readily available commercialized software, targeting on the micro-scale fluid and polymerization mechanics that are relevant to the extrinsic self-healing polymeric system is worth to be explored considering no relevant work is reported in the literature thus far. Specifically, the framework should survive necessitated numerical verifications before further assessment can be conducted tailoring for the synthetic system design.

On one hand, the penalty finite element formulation for incompressible Stokes approximation is an ideal computational tool for simplistic fluid flow simulation (Zhou, 2012; Reddy and Gartling, 2010; Zienkiewicz et al., 2014). On the other hand, the basic energy flow is governed by the Fourier's law where relevant disturbance on the heat equilibrium due to the curing phenomenon, say involving polymeric liquid, could be simplistically represented by coupling phenomenological-based approach to the finite element formulation (Zhou, 2012; Reddy and Gartling, 2010; Zienkiewicz et al., 2013). Despite popularity of both formulations within the computational realm, a firm and unified set of guidelines in tackling the companion numerical issues (e.g. stability, consistency, and accuracy) when employing the weak form Galerkin finite element method as the base numerical framework remains under-developed (Bathe, 1996; Reddy and Gartling, 2010; Zienkiewicz et al., 2013, 2014) and hence a research gap worthy of special consideration in the present study.

To achieve the best repairing effect, the search of the optimal chemistry often begins with the fastest possible cure rate. Nevertheless, such chemistry is often accompanied by the relative extreme exothermic peak that is detrimental to the formation of the adhesive repair due to the induced residual stresses/distortions (Zhang and Rong, 2011; Zhou, 2012; Binder, 2013). Such damage healing invokes

a non-favorable strength restoration and shall constitute as one of the core criterions under the scope of solid-polymerization consideration (i.e. Zone II-2 in Figure 1.5). Adherent to the limited awareness of this mutual contribution in the self-healing polymer literature, the development of an evaluator system targeted on capturing these inter-linked characteristics based on the weak form Galerkin finite element model is lacking and worth to be explored.

### **1.3 Objectives of the Study**

The examination of the fluid and polymerization mechanics as well as the search of the optimal strength recovery system through respective numerical setting, preferably in a stable and concise environment but yet at an affordable computational framework, is highly desirable considering the inherent multi-physics and multi-scales nature of the external self-healing practice. It is the aim of the present study to accomplish such efforts through the self-developed in-house MATLAB algorithms, the objectives of which include:

- (A) To formulate a discrete Stokes model in micro-scaled fluid setting by coupling the weak form Galerkin finite element method and penalty function method.
- (B) To determine the suitable numerical techniques and associated optimal parameters for the efficient use of model from Objective (A) in both steady and transient simulations.
- (C) To formulate a phenomenological-based polymerization model that couples to the heat conduction analysis by using the weak form Galerkin finite element method.
- (D) To determine the key kinetic parameters of the healing epoxy in fulfilling the polymerization optimality based on the model from Objective (C).

### **1.4 Scopes of the Study**

The multi-physics and multi-scales nature of the external self-healing practice in polymeric materials impose numerous potential scopes for study. The fracture mechanics is first excluded from consideration by limiting the present work to a readily formed crack geometry as schematically given in Figure 1.4 (b). Both fluid

and polymerization mechanics considered for the model are presumed to be bounded in a micro-scaled horizontal domain (refer Figure 1.4 (c)) as given in Figure 1.6 (a). Hence, the macro-scale undamaged portion is negligible.

Furthermore, the focus of relevant mechanics in 1D domain is adopted in the present study as presented in Figure 1.6 (b) due to the feasibility of dominantly unidirectional assumption (Reddy, 2006; Zienkiewicz et al., 2013) if the cross-sectional dimension (i.e.  $\mu\text{m}$  scale) is sufficiently small than that of length (i.e. mm scale). Moreover, the fluid and polymerization mechanics are considered separately in the present study to avoid the potential numerical complexity due to the multi-physics concern (Bathe, 1996; Reddy and Gartling, 2010). As a matter of fact, the time scale ( $t$ ) for fluid mechanics is often much shorter than that of the polymerization (refer response-time plot of synthetic system in Figure 1.3) due to the optimal infiltration rate requirement and hence the assumption of no obvious non-linearity overlapping concern among these mechanics is justified.

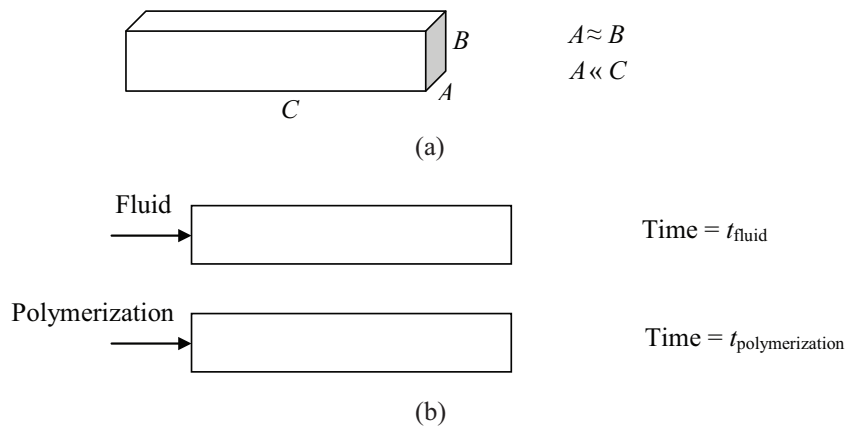


**Figure 1.6:** The domain of (a) presume crack geometry and (b) fluid flow and polymerization.

The scopes relevant to the hydrodynamics aspects in the present study include:

- (a) Flow nature
  - (i) Laminar flow.
  - (ii) Flow length  $< 20\text{mm}$ .
  - (iii) Micro-channel ( $10\mu\text{m} - 200\mu\text{m}$ ) (Kandlikar et al., 2005).

- (iv) Inlet velocity  $< 5\text{m/s}$ .
  - (v) Atmospheric outlet pressure.
  - (vi) Viscous incompressible Newtonian fluid.
- (b) Modeling framework
- (i) Stokes equations.
  - (ii) Velocity and pressure variables.
  - (iii) Weak form Galerkin finite element method.
  - (iv) Consistent penalty function method.
  - (v) Lagrangian shape functions (i.e. quadratic and linear).
  - (vi) Crank Nicolson predictor-corrector time integration scheme.

On the other hand, the scopes relevant to the thermodynamics as well as polymerization aspects in the present study are:

- (a) Heat transfer nature
- (i) Heat conduction.
  - (ii) Neumann inlet boundary (i.e. zero heat influx).
  - (iii) Dirichlet outlet boundary (i.e. constant temperature).
  - (iv) Phenomenological polymerization (Kessler and White, 2002; Zhou, 2012).
- (b) Modeling framework
- (i) Fourier's law.
  - (ii) Temperature and cure degree variables.
  - (iii) Weak form Galerkin finite element method.
  - (iv) Lagrangian shape function (i.e. linear).
  - (v) Crank-Nicolson time integration scheme.
  - (vi) Arrhenius's rate equation (Kessler and White, 2002; Zhou, 2012).

## 1.5 Significance of the Study

Two typical in-house weak form Galerkin finite element models targeted on capturing fluid dynamics and thermodynamics response are developed in the present study, respectively. Equipped with considerable numerical validation and verification, along with specific remedies to deal with the prompted underlying computational issues, these models are readily adopted to assess the infiltration and polymerization behaviors of the infilling polymeric liquid in single unidirectional crack geometry.

Besides, the output of these in-house models (e.g. velocity, pressure, evolution of both temperature as well as the cure degree) readily serves as the input parameters for both the structural and fracture module (refer Figure 1.5) in order to accomplish the core mechanics assessment of extrinsic self-healing mechanisms in polymeric materials. Specifically, the infilling behavior offers the details on the remaining crack portion that contribute nothing to structural strength and perhaps the next crack origin. On the other hand, the polymerization behavior (i.e. the axial cure degree along the unidirectional crack domain) offers the relevant information on the strength gain throughout the healed event to cater the next fracture.

Generally, a thorough and representative mechanical assessment on the optimality of the healing performance in a single realistic crack geometry is readily achievable based on the output parameters generated by the in-house weak form Galerkin finite element models developed in the present study. Note that relevant work on this aspect remains lacking in the literature. Several companion benefits throughout the development of the in-house weak form Galerkin finite element models are highlighted herein:

- (a) The experience in numerical validating and verifying these models could be laid as the reference framework to develop much advanced infiltration and polymerization module corresponding to the much realistic crack phenomenon (i.e. 2D/3D spanning as well as multiple branches) and polymer chemistry.
- (b) The survival of the weak form Galerkin finite element fluid flow and heat transfer module from the computational issues encourages a unified numerical framework to be developed targeted on extrinsic self-healing mechanisms. Specifically, the transfer of the multi-physics variable under similar numerical method is convenient and favorable. Therefore, the effort contributed in the present study shall serve as a milestone for the upcoming research in this realm.

- (c) The benefit of coupling examination of multi-physics variable is demonstrated in the present study. Particularly, the unification of both temperature and cure degree evolution under a single evaluator is demonstrated to work ideally in assessing the solid-polymerization mechanics. Much representative and crucial examination in similar trend is expected shall the unified weak form Galerkin finite element framework is readily developed to assess the underlying multi-physics variables (i.e. stress, strains, velocity, pressure, temperature, cure degree, and etc.) embedded in the damage-transport-chemical repair of the extrinsic self-healing mechanisms in self-healing polymeric materials.

The relevant numerical difficulties, with respect to each independent aspect of diffusive fluid and energy flow, are demonstrated and solved within the limited scopes of the present study in the 1D domain. Specifically, two categories of discussion mainly on computational mechanics aspect are presented both theoretically and practically:

- (a) Effective use of penalty function method in solving both steady and transient incompressible Stokes equations
- (i) Demonstrate penalty parameter ( $\gamma_p$ )-spatial mesh ( $\Delta x$ ) relation in terms of numerical stability, consistency, and accuracy.
  - (ii) Demonstrate the role of elemental divergence of velocity (EDV) components corresponding to mass conservation in both iterative penalty setting and modified iterative penalty setting.
- (b) Demonstrate the problematic coupling of weak form Galerkin finite element spatial discretization and single-step finite difference temporal discretization in capturing the dynamic behaviors of diffusive fluid motion and diffusive energy transfer
- (i) Highlight on erroneous perspective that numerical stability, consistency, and accuracy is ensured as long as there is a sufficient mesh refinement (i.e. spatial, temporal, and both).
  - (ii) Establish the  $\Delta x$ -temporal mesh ( $\Delta t$ ) relation for efficient penalty fluid flow simulation

## 1.6 Outlines of the Thesis

This thesis comprises seven chapters. After the present introductory chapter, Section 2.1 focuses on the recent practical developments in self-healing polymeric materials, particularly those adopt external/extrinsic-based healing system. The key mechanics in the extrinsic self-healing mechanisms, namely fluid and polymerization, that are worth to be examined numerically are highlighted in Section 2.2. Relevant numerical issues and potential remedy, both steady and transient, if the FE Eulerian framework is adopted is then discussed in Section 2.3. The nature and scopes of the present study are then aligned with the main research issues stated throughout the previous discussions and listed in Section 2.4.

Section 3.1 and Section 3.2 present the main governing equations for the incompressible fluid flow and polymerization models in the present study, respectively. Generally, the weak form Galerkin formulations for both models along with their appropriate boundary conditions are given where the development ranging from the selection of shape functions to the assembly of the matrix system and later the solution procedure are discussed. Several expected findings from these models are highlighted in Section 3.3.

The pressure solutions in a straight micro-channel based on the FE incompressible fluid flow model are presented in Section 4.1. A beneficial remedy framework, based on the iterative penalty Galerkin FE setting, in terms of numerical stability and consistency is highlighted in Section 4.2. The optimal coupling between spatial mesh size and the penalty parameter for numerical accuracy is tested and a preliminary benchmark range is proposed in Section 4.3. A modified framework is later proposed in Section 4.4 due to the numerical deficiency of the benchmark range where the stability, consistency, and accuracy of the pressure solution based on the new framework are demonstrated. Several recommendations beneficial to the development of penalty Galerkin FE incompressible fluid flow model are summarized in Section 4.5.

The pressure solution resulted from the integration of the predictor-corrector temporal scheme to the penalty Galerkin FE model is presented in Section 5.1. The optimal coupling between the temporal mesh size and the penalty parameter is later tested in Section 5.2 for a wide range of the channel geometries and inflow conditions, most of which aligned to the extrinsic self-healing practice, where a parameter targeted for optimal stability, consistency, and accuracy of the pressure solutions is given.

Satisfactory performance of the parameter is later demonstrated for the flow front tracking in micro-channel along with the progression of the pressure distribution. The main guidelines beneficial to the development of transient penalty Galerkin FE incompressible fluid model are summarized in Section 5.3.

The steady heat conduction modeling with heat generation term is presented in Section 6.1 whereas extension of the framework aligned to the heat release due to the polymerization is given in Section 6.2. The heat generation and cure rates based on the polymerization kinetics adopted in Yuan et al. (2009) are evaluated in Section 6.3 where an useful relation between the temperature as well as cure evolution and the strength recovery performance of the self-healing specimen is proposed. Performance charts are generated in Section 6.4 from the parametric study adopting the key kinetic components of the epoxy healant where the main direction towards the optimal mechanical recovery is demonstrated. The beneficial search of the optimal mechanical performance based on the numerical framework is highlighted in Section 6.5.

Section 7.1 summarizes the main findings from the numerical solutions (e.g. velocity, pressure, temperature and cure degree) generated from the FE models in the present study where appropriate guidelines that ensure stability, consistency, and accuracy are listed. The postulated strength recovery, based on the numerical evaluation of both the temperature and cure degree evolution, as a simple tool beneficial to the optimal search of the self-healing polymer chemistry as presented in the present study is highlighted. Several recommendations aligning to the extrinsic self-healing practice in polymeric materials that are worth to be extended under the accomplishment of the scopes in the present study are also given.



## REFERENCES

- Aïssa, B., Therriault, D., Haddad, E., and Jamroz, W. (2012). Self-healing materials systems: Overview of major approaches and recent developed technologies. *Advances in Materials Science and Engineering*, 2012:Article ID 854203.
- Akira, M. (1994). Element-by-element penalty/uzawa formulation for large scale flow problems. *Computer Methods in Applied Mechanics and Engineering*, 112(1):283–289.
- Aldridge, M., Wineman, A., Waas, A., and Kieffer, J. (2014). In situ analysis of the relationship between cure kinetics and the mechanical modulus of an epoxy resin. *Macromolecules*, 47(23):8368–8376.
- Alharbi, A. Y., Pence, D. V., and Cullion, R. N. (2003). Fluid flow through microscale fractal-like branching channel networks. In *ASME 2003 1st International Conference on Microchannels and Minichannels*, pages 869–877. American Society of Mechanical Engineers.
- Alsheghri, A. A. and Al-Rub, R. K. A. (2016). Finite element implementation and application of a cohesive zone damage-healing model for self-healing materials. *Engineering Fracture Mechanics*, 163:1–22.
- Babuška, I. (1973). The finite element method with lagrangian multipliers. *Numerische Mathematik*, 20(3):179–192.
- Bathe, K.-J. (1996). *Finite Element Procedures*. New Jersey:Prentice-Hall.
- Behzad, T. and Sain, M. (2007). Finite element modeling of polymer curing in natural fiber reinforced composites. *Composites Science and Technology*, 67(7):1666–1673.
- Bercovier, M. and Engelman, M. (1979). A finite element for the numerical solution of viscous incompressible flows. *Journal of Computational Physics*, 30(2):181–201.
- Billiet, S., Hillewaere, X. K., Teixeira, R. F., and Du Prez, F. E. (2013). Chemistry of crosslinking processes for self-healing polymers. *Macromolecular Rapid Communications*, 34(4):290–309.
- Binder, W. H. (2013). *Self-Healing Polymers: From Principles to Applications*. Weinheim:John Wiley and Sons.

- Blaiszik, B., Kramer, S., Olugebefola, S., Moore, J. S., Sottos, N. R., and White, S. R. (2010). Self-healing polymers and composites. *Annual Review of Materials Research*, 40:179–211.
- Bluhm, J., Specht, S., and Schröder, J. (2015). Modeling of self-healing effects in polymeric composites. *Archive of Applied Mechanics*, 85(9-10):1469–1481.
- Brezzi, F. (1974). On the existence, uniqueness and approximation of saddle-point problems arising from lagrangian multipliers. *Revue française d'automatique, informatique, recherche opérationnelle. Analyse numérique*, 8(2):129–151.
- Brown, E. N., White, S. R., and Sottos, N. R. (2005). Retardation and repair of fatigue cracks in a microcapsule toughened epoxy composite part ii: In situ self-healing. *Composites Science and Technology*, 65(15):2474–2480.
- Carey, G. and McLay, R. (1986). Local pressure oscillation and boundary treatment for the 8-node quadrilateral. *International Journal for Numerical Methods in Fluids*, 6(3):165–172.
- Chen, J., Pan, C., and Chang, T. (1995). On the control of pressure oscillation in bilinear-displacement constant-pressure element. *Computer Methods in Applied Mechanics and Engineering*, 128(1-2):137–152.
- Engelman, M., Sani, R., Gresho, P., and Bercovier, M. (1982). Consistent vs. reduced integration penalty methods for incompressible media using several old and new elements. *International Journal for Numerical Methods in Fluids*, 2(1):25–42.
- Engelman, M. S. (1982). Fidap (a fluid dynamics analysis program). *Advances in Engineering Software (1978)*, 4(4):163–166.
- Everitt, D. T., Luterbacher, R., Coope, T. S., Trask, R. S., Wass, D. F., and Bond, I. P. (2015). Optimisation of epoxy blends for use in extrinsic self-healing fibre-reinforced composites. *Polymer*, 69:283–292.
- Faragó, I. and Horváth, R. (2007). A review of reliable numerical models for three-dimensional linear parabolic problems. *International Journal for Numerical Methods in Engineering*, 70(1):25–45.
- Fortin, M. and Glowinski, R. (1983). *Augmented Lagrangian Methods: Applications to the Numerical Solution of Boundary-value Problems*. Oxford:Elsevier.
- Fox, R. W., McDonald, A. T., and Pritchard, P. J. (2004). *Introduction to Fluid Mechanics (Sixth Edition)*. Hoboken:John Wiley and Sons.
- Ghazali, H., Ye, L., and Zhang, M. Q. (2016). Interlaminar fracture of cf/ep composite containing a dual-component microencapsulated self-healant. *Composites Part A: Applied Science and Manufacturing*, 82:226–234.

- Ghosh, S. K. (2009). *Self-Healing Materials: Fundamentals, Design Strategies, and Applications*. Weinheim:John Wiley and Sons.
- Gresho, P. M. and Lee, R. L. (1981). Don't suppress the wiggles - they're telling you something! *Computers and Fluids*, 9(2):223–253.
- Gresho, P. M. and Sani, R. L. (1998). *Incompressible Flow and The Finite Element Method. Volume 1: Advection-Diffusion and Isothermal Laminar Flow*. New York:John Wiley and Sons.
- Hall, J., Qamar, I., Rendall, T., and Trask, R. (2015). A computational model for the flow of resin in self-healing composites. *Smart Materials and Structures*, 24(3):037002.
- Hillewaere, X. K. and Du Prez, F. E. (2015). Fifteen chemistries for autonomous external self-healing polymers and composites. *Progress in Polymer Science*, 49:121–153.
- Hughes, T. J. (1987). *The Finite Element Method: Linear Static and Dynamic Finite Element Analysis*. Englewood Cliffs: Prentice-Hall.
- Hughes, T. J., Liu, W. K., and Brooks, A. (1979). Finite element analysis of incompressible viscous flows by the penalty function formulation. *Journal of Computational Physics*, 30(1):1–60.
- Huyakorn, P., Taylor, C., Lee, R., and Gresho, P. (1978). A comparison of various mixed-interpolation finite elements in the velocity-pressure formulation of the navier-stokes equations. *Computers and Fluids*, 6(1):25–35.
- Jones, A. and Dutta, H. (2010). Fatigue life modeling of self-healing polymer systems. *Mechanics of Materials*, 42(4):481–490.
- Kandlikar, S., Garimella, S., Li, D., Colin, S., and King, M. R., editors (2005). *Heat Transfer and Fluid Flow in Minichannels and Microchannels*. Oxford:Elsevier.
- Kessler, M. R. and White, S. R. (2002). Cure kinetics of the ring-opening metathesis polymerization of dicyclopentadiene. *Journal of Polymer Science Part A: Polymer Chemistry*, 40(14):2373–2383.
- Krull, B. P., Gergely, R. C., Santa Cruz, W. A., Fedonina, Y. I., Patrick, J. F., White, S. R., and Sottos, N. R. (2016). Strategies for volumetric recovery of large scale damage in polymers. *Advanced Functional Materials*, 26(25):4561–4569.
- Ladyzhenskaya, O. A. and Silverman, R. A. (1969). *The Mathematical Theory of Viscous Incompressible Flow (Second Edition)*. New York:Gordon and Breach.
- Lewis, R. W., Nithiarasu, P., and Seetharamu, K. N. (2004). *Fundamentals of the Finite Element Method for Heat and Fluid flow*. Chichester:John Wiley and Sons.

- Li, G. and Meng, H. (2015). *Recent Advances in Smart Self-Healing Polymers and Composites*. Oxford:Elsevier.
- Liu, X., Lee, J. K., Yoon, S. H., and Kessler, M. R. (2006). Characterization of diene monomers as healing agents for autonomic damage repair. *Journal of Applied Polymer Science*, 101(3):1266–1272.
- Liu, X., Sheng, X., Lee, J. K., Kessler, M. R., and Kim, J. S. (2009). Rheokinetic evaluation of self-healing agents polymerized by grubbs catalyst embedded in various thermosetting systems. *Composites Science and Technology*, 69(13):2102–2107.
- Mauldin, T. C., Leonard, J., Earl, K., Lee, J. K., and Kessler, M. R. (2012). Modified rheokinetic technique to enhance the understanding of microcapsule-based self-healing polymers. *ACS Applied Materials and Interfaces*, 4(3):1831–1837.
- Meng, H. and Li, G. (2013). A review of stimuli-responsive shape memory polymer composites. *Polymer*, 54(9):2199–2221.
- Mizukami, A. (1985). Finite element analysis of the steady navier-stokes equations by a multiplier method. *International Journal for Numerical Methods in Fluids*, 5(3):281–292.
- Murphy, E. B. and Wudl, F. (2010). The world of smart healable materials. *Progress in Polymer Science*, 35(1):223–251.
- Park, H. C., Goo, N. S., Min, K. J., and Yoon, K. J. (2003). Three-dimensional cure simulation of composite structures by the finite element method. *Composite Structures*, 62(1):51–57.
- Park, H. C. and Lee, S. W. (2001). Cure simulation of thick composite structures using the finite element method. *Journal of Composite Materials*, 35(3):188–201.
- Patrick, J. F., Robb, M. J., Sottos, N. R., Moore, J. S., and White, S. R. (2016). Polymers with autonomous life-cycle control. *Nature*, 540(7633):363–370.
- Pelletier, D., Fortin, A., and Camarero, R. (1989). Are fem solutions of incompressible flows really incompressible? (or how simple flows can cause headaches!). *International Journal for Numerical Methods in Fluids*, 9(1):99–112.
- Pence, D. (2003). Reduced pumping power and wall temperature in microchannel heat sinks with fractal-like branching channel networks. *Microscale Thermophysical Engineering*, 6(4):319–330.
- Rabearison, N., Jochum, C., and Grandidier, J.-C. (2009). A fem coupling model for properties prediction during the curing of an epoxy matrix. *Computational Materials Science*, 45(3):715–724.

- Reddy, J. (1982). On penalty function methods in the finite-element analysis of flow problems. *International Journal for Numerical Methods in Fluids*, 2(2):151–171.
- Reddy, J. N. (2006). *An Introduction to the Finite Element Method (Third Edition)*. New York:McGraw-Hill.
- Reddy, J. N. and Gartling, D. K. (2010). *The Finite Element Method in Heat Transfer and Fluid Dynamics*. Boca Raton:CRC press.
- Reddy, M., Reddy, J., and Akay, H. (1992). Penalty finite element analysis of incompressible flows using element by element solution algorithms. *Computer Methods in Applied Mechanics and Engineering*, 100(2):169–205.
- Reddy, M., Reifschneider, L., Reddy, J., and Akay, H. (1993). Accuracy and convergence of element-by-element iterative solvers for incompressible fluid flows using penalty finite element model. *International Journal for Numerical Methods in Fluids*, 17(12):1019–1033.
- Rouison, D., Sain, M., and Couturier, M. (2003). Resin-transfer molding of natural fiber-reinforced plastic. i. kinetic study of an unsaturated polyester resin containing an inhibitor and various promoters. *Journal of Applied Polymer Science*, 89(9):2553–2561.
- Rouison, D., Sain, M., and Couturier, M. (2004). Resin transfer molding of natural fiber reinforced composites: Cure simulation. *Composites Science and Technology*, 64(5):629–644.
- Ruiz, E. and Trochu, F. (2005). Comprehensive thermal optimization of liquid composite molding to reduce cycle time and processing stresses. *Polymer Composites*, 26(2):209–230.
- Ruiz, E. and Trochu, F. (2006). Multi-criteria thermal optimization in liquid composite molding to reduce processing stresses and cycle time. *Composites Part A: Applied Science and Manufacturing*, 37(6):913–924.
- Saha, A. A. and Mitra, S. K. (2008). Modeling and simulation of microscale flows. In Petrone, G. and Cammarate, G., editors, *Modelling and Simulation*, pages 283–316. Rijeka: Intech.
- Schimmel, E. and Remmers, J. (2006). Development of a constitutive model for self-healing materials. *Report DACS-06-003*.
- Shojaei, A., Sharafi, S., and Li, G. (2015). A multiscale theory of self-crack-healing with solid healing agent assisted by shape memory effect. *Mechanics of Materials*, 81:25–40.
- Struzziero, G. and Skordos, A. A. (2017). Multi-objective optimisation of the cure of

- thick components. *Composites Part A: Applied Science and Manufacturing*, 93:126–136.
- Trask, R., Williams, G., and Bond, I. (2007). Bioinspired self-healing of advanced composite structures using hollow glass fibres. *Journal of the Royal Society Interface*, 4(13):363–371.
- Tsangouri, E., Aggelis, D., and Van Hemelrijck, D. (2015). Quantifying thermoset polymers healing efficiency: A systematic review of mechanical testing. *Progress in Polymer Science*, 49:154–174.
- Wang, W., Li, X., and Han, X. (2012). Numerical simulation and experimental verification of the filling stage in injection molding. *Polymer Engineering and Science*, 52(1):42–51.
- Wang, Y., Pham, D. T., and Ji, C. (2015). Self-healing composites: A review. *Cogent Engineering*, 2(1):1075686.
- White, F. M. and Corfield, I. (2006). *Viscous Fluid Flow (Third Edition)*. New York:McGraw-Hill.
- White, S., Moore, J., Sottos, N., Krull, B., Santa Cruz, W., and Gergely, R. (2014). Restoration of large damage volumes in polymers. *Science*, 344(6184):620–623.
- White, S. R., Sottos, N., Geubelle, P., Moore, J., Kessler, M., Sriram, S., Brown, E., and Viswanathan, S. (2001). Autonomic healing of polymer composites. *Nature*, 409(6822):794–797.
- Wu, D. Y., Meure, S., and Solomon, D. (2008). Self-healing polymeric materials: A review of recent developments. *Progress in Polymer Science*, 33(5):479–522.
- Yang, C. and Gu, Y. (2006). Minimum time-step criteria for the galerkin finite element methods applied to one-dimensional parabolic partial differential equations. *Numerical Methods for Partial Differential Equations*, 22(2):259–273.
- Yang, G. and Lee, J. K. (2014). Curing kinetics and mechanical properties of endodicyclopentadiene synthesized using different grubbs catalysts. *Industrial and Engineering Chemistry Research*, 53(8):3001–3011.
- Yang, Y., Ding, X., and Urban, M. W. (2015). Chemical and physical aspects of self-healing materials. *Progress in Polymer Science*, 49:34–59.
- Yi, S., Hilton, H. H., and Ahmad, M. F. (1997). A finite element approach for cure simulation of thermosetting matrix composites. *Computers and Structures*, 64(1-4):383–388.
- Yuan, Y., Yin, T., Rong, M., and Zhang, M. (2008). Self healing in polymers and polymer composites. concepts, realization and outlook: A review. *eXPRESS*

- Polymer Letters*, 2(4):238–250.
- Yuan, Y. C., Rong, M. Z., Zhang, M. Q., and Yang, G. C. (2009). Study of factors related to performance improvement of self-healing epoxy based on dual encapsulated healant. *Polymer*, 50(24):5771–5781.
- Zeng, J. (2007). On modeling of capillary filling. Technical report.
- Zhang, M. Q. and Rong, M. Z. (2011). *Self-Healing Polymers and Polymer Composites*. New Jersey:John Wiley and Sons.
- Zhang, P. and Li, G. (2016). Advances in healing-on-demand polymers and polymer composites. *Progress in Polymer Science*, 57:32–63.
- Zhou, H. (2012). *Computer modeling for injection molding: simulation, optimization, and control*. John Wiley & Sons.
- Zhu, D. Y., Rong, M. Z., and Zhang, M. Q. (2015). Self-healing polymeric materials based on microencapsulated healing agents: From design to preparation. *Progress in Polymer Science*, 49:175–220.
- Zienkiewicz, O., Taylor, R., and Zhu, J. (2013). *The Finite Element Method: Its Basis and Fundamentals*. Oxford:Butterworth-Heinemann.
- Zienkiewicz, O. and Löhner, R. (1985). Accelerated relaxation or direct solution? future prospects for fem. *International Journal for Numerical Methods in Engineering*, 21(1):1–11.
- Zienkiewicz, O., Qu, S., Taylor, R., and Nakazawa, S. (1986). The patch test for mixed formulations. *International Journal for Numerical Methods in Engineering*, 23(10):1873–1883.
- Zienkiewicz, O., Taylor, R., and Nithiarasu, P. (2014). *The Finite Element Method for Fluid Dynamics (Seventh Edition)*. Oxford:Butterworth-Heinemann.
- Zienkiewicz, O., Vilotte, J.-P., Toyoshima, S., and Nakazawa, S. (1985). Iterative method for constrained and mixed approximation. an inexpensive improvement of fem performance. *Computer Methods in Applied Mechanics and Engineering*, 51(1-3):3–29.
- Zwaag, S. (2007). *Self Healing Materials: An Alternative Approach to 20 Centuries of Materials Science*. Dordrecht:Springer.